Tailoring the Surface and Solubility Properties of Nanocrystalline Titania by a Nonaqueous In Situ Functionalization Process

Markus Niederberger,*,† Georg Garnweitner,† Frank Krumeich,‡ Reinhard Nesper,‡ Helmut Cölfen,† and Markus Antonietti†

Max-Planck-Institute of Colloids and Interfaces, D-14424 Potsdam, Germany, and Laboratory of Inorganic Chemistry, Swiss Federal Institute of Technology (ETH), ETH Hönggerberg-HCI, CH-8093 Zürich, Switzerland

Received August 1, 2003. Revised Manuscript Received January 8, 2004

The reaction between titanium tetrachloride and benzyl alcohol in the presence of enediol ligands such as dopamine and 4-*tert*-butylcatechol provides a simple nonaqueous route to in situ surface functionalization of titania nanoparticles. The as-prepared precipitates are resoluble either in water or in organic solvents, depending on the ligand used. The surface chemistry of the 4-*tert*-butylcatechol-functionalized particles dissolved in dimethylformamide was analyzed by ^{1}H NMR measurements revealing the presence of adsorbed 4-*tert*-butylcatechol, in addition to benzyl alcohol and water. Although the reaction temperatures of 70 or 80 °C are relatively low, XRD and HRTEM investigations give evidence that the as-synthesized nanoparticles are highly crystalline. Ultracentrifugation analysis of dopamine-functionalized titania nanoparticles dissolved in water shows a particle size distribution of approximately 3.5−8 nm with the peak maximum at 5.5 nm. Furthermore, the UV−vis detector system of the ultracentrifuge allows the measurement of the absorption spectra dependent on the particle size, showing an unusual red shift with decreasing particle size.

Introduction

In the past few years, a main objective of nanochemistry was the development of improved methods for the synthesis and characterization of nanoparticles with a strong focus on the control over particle size, shape, size distribution, and crystallinity. More recently, a new trend has been established with the aim of arranging individual nanoparticles into hierarchically ordered superstructures via self-assembly and investigating the collective properties resulting from the interaction of the particles.[1] Self-assembly is one of the few practical strategies for making ensembles of nanostructures and, thus, will be an essential part of nanotechnology.[2]

The proper design of the individual components that organize themselves into desired patterns and functions is the key to applications of self-assembly. In most cases, self-assembly requires that the building units are mobile and therefore, it takes place in fluid phases or on smooth surfaces. There is no doubt that adequately tailored surface properties are the fundamental parameter in the design of novel nanobuilding blocks. The surface properties determine the interactions among the components, as well as the solubility and agglomeration behavior in different solvents and, thus, decide whether individual nanoparticles are suitable as nanobuilding blocks for the design of nanocomposites or for self-organizing nanodevices.[3]

In addition to potential applications in mesoscale self-assembly processes, functionalized nanoparticles already play an important role in the synthesis of hybrid organic−inorganic nanocomposites,[4−7] in the photodegradation of organic pollutants[8−10] and heavy metals,[11] and in the preparation of organic−inorganic hybrid catalysts.[12] To connect the inorganic building blocks to the organic moiety in hybrid materials by strong covalent or ionic interactions, reactive organic groups have to be attached onto the surface of the inorganic component. There are two general surface modification methods, either the grafting of organic groups to a preformed nanoparticle (postsynthesis modification) or introduction during the nanoparticle synthesis (in situ modification).[13,14] The advantage of the in situ functionalization

* Corresponding author. E-mail: markus.niederberger@mpikg-golm.mpg.de.
† Max-Planck-Institute of Colloids and Interfaces.
‡ Swiss Federal Institute of Technology (ETH).

(1) Weller, H. *Angew. Chem.-Int. Ed.* **1996**, *35*, 1079−1081.
(2) Whitesides, G. M.; Grzybowski, B. *Science* **2002**, *295*, 2418−2421.
(3) Shenhar, R.; Rotello, V. M. *Acc. Chem. Res.* **2003**, *36*, 549−561.
(4) Wen, J.; Wilkes, G. L. *Chem. Mater.* **1996**, *8*, 1667−1681.
(5) Pomogailo, A. D. *Russ. Chem. Rev.* **2000**, *69*, 53−80.
(6) Gangopadhyay, R.; De, A. *Chem. Mater.* **2000**, *12*, 608−622.
(7) Gomez-Romero, P. *Adv. Mater.* **2001**, *13*, 163−174.
(8) Makarova, O. V.; Rajh, T.; Thurnauer, M. C.; Martin, A.; Kemme, P. A.; Cropek, D. *Environ. Sci. Technol.* **2000**, *34*, 4797−4803.
(9) Shchukin, D. G.; Schattka, J. H.; Antonietti, M.; Caruso, R. A. *J. Phys. Chem. B* **2003**, *107*, 952−957.
(10) Schattka, J. H.; Shchukin, D. G.; Jia, J. G.; Antonietti, M.; Caruso, R. A. *Chem. Mater.* **2002**, *14*, 5103−5108.
(11) Chen, L. X.; Rajh, T.; Wang, Z. Y.; Thurnauer, M. C. *J. Phys. Chem. B* **1997**, *101*, 10688−10697.
(12) Wight, A. P.; Davis, M. E. *Chem. Rev.* **2002**, *102*, 3589−3614.
(13) Kickelbick, G.; Schubert, U. In *Synthesis, Functionalization and Surface Treatment of Nanoparticles*; Baraton, M.-I., Ed.; American Scientific Publishers: Stevenson Ranch, CA, 2003.
(14) Sanchez, C.; Soler-Illia, G.; Ribot, F.; Lalot, T.; Mayer, C. R.; Cabuil, V. *Chem. Mater.* **2001**, *13*, 3061−3083.

10.1021/cm031108r CCC: $27.50 © 2004 American Chemical Society
Published on Web 02/28/2004

lies in the self-limiting organization process of the inorganic and organic building blocks, where on one hand the organic ligand controls the growth of the nanoparticle and, on the other hand, the attachment of the organic group on the nanoparticle surface is governed by the chemical reactions that result in the formation of the nanoparticles.[13]

Titanium dioxide is a material with outstanding chemical and physical properties, which are of interest for a wide variety of different applications in gas sensing,[15,16] catalysis,[17] photocatalysis,[18−20] optics,[21,22] photovoltaics,[23,24] and pigmentation.[25] Our synthesis approach reported here is based on a nonaqueous sol−gel process using benzyl alcohol as solvent and titanium tetrachloride as titanium oxide precursor at low temperatures. Benzyl alcohol has proven to be a versatile reaction medium for the synthesis of crystalline transition-metal oxide nanoparticles.[26,27] In addition, there is no safety concern for benzyl alcohol; the substance may be used in foodstuffs and fragrances.

Central to our approach is the in situ tailoring of the surface properties of the titania nanoparticles by suitable functional groups covalently attached to the surface of the particles. The colloidal route for the synthesis of titania nanoparticles has commonly been employed, since surface modification can be easily accomplished in solution.[28−32] It has been reported that enediol ligands such as ascorbic acid, catechol, dopamine, and alizarin bind to transition metal oxides via covalent linkage,[33−35] providing a facile means of modifying the surface of the nanoparticles with specific functional groups. Also, siderophores with catechol end groups bind covalently to titanium oxide.[36]

In this work, in situ modification of the surface of the titania particles was performed by the addition of titanium tetrachloride to a mixture of benzyl alcohol and dopamine or 4-*tert*-butylcatechol. In contrast to previously reported colloidal routes, our approach results in the formation of resoluble precipitates rather than a stable colloidal solution. It is a notable feature of the benzyl alcohol solvent that both the dopamine-functionalized as well as the 4-*tert*-butylcatechol-functionalized nanoparticles form a precipitate. Depending on the functionalization, the as-synthesized titania particles are soluble either in water or in organic solvents such as tetrahydrofuran, dimethylformamide, and dimethyl sulfoxide. Furthermore, the solubility of the as-synthesized nanoparticles simplifies analysis of particle size and distribution by analytical ultracentrifugation.[37] In contrast to methods such as TEM, where information about the particle size distribution is obtained only from a very restricted subset of the sample, ultracentrifugation provides statistical information about the whole sample. Physical properties such as band gap energies of various particle fractions can easily be measured within the AUC (analytical ultracentrifugation) run,[38] giving information about the dependence of physical properties on the particle size.

Results and Discussion

In the first step of the synthesis, titanium tetrachloride is added dropwise and under vigorous stirring to a mixture of benzyl alcohol and dopamine or 4-*tert*-butylcatechol. Dopamine forms a cloudy suspension in benzyl alcohol, whereas 4-*tert*-butylcatechol is soluble. The dark red reaction mixture is aged at room temperature for about 2 h and subsequently heated to either 70 °C for 4-*tert*-butylcatechol or 80 °C for dopamine for 2−5 days. The product is recovered by centrifugation. Subsequent washing with chloroform or methylene chloride and drying at 60 °C led to a brown powder in good yield (Figure 1a). The dried dopamine-coated titania powder can easily be redissolved in water, resulting in a red, completely transparent solution (Figure 1b). Surface-modification with dopamine ligands having positively charged terminal ammonium groups results in particle−particle repulsion and leads to a stable aqueous colloidal solution.[33] The still wet and freshly prepared 4-*tert*-butylcatechol-functionalized sample has to be directly redissolved in tetrahydrofuran (THF), dimethylformamide (DMF), or dimethyl sulfoxide (DMSO) after the removal of the benzyl alcohol, because the washed and dried powder is less soluble. This fact is due to the enhanced particle−particle interaction, since surface modification with 4-*tert*-butylcatechol eliminates the surface charge.[33] However, a postsynthesis treatment of the as-synthesized, wet particles in differently concentrated solutions of 4-*tert*-butylcatechol in chloroform increases the solubility properties of the dried powder by saturating the surface of the titania nanoparticles with the 4-*tert*-butylcatechol ligands. Furthermore, also the addition of a small amount of

(15) Traversa, E.; Di Vona, M. L.; Licoccia, S.; Sacerdoti, M.; Carotta, M. C.; Crema, L.; Martinelli, G. *J. Sol-Gel Sci. Technol.* **2001**, *22*, 167−179.
(16) Guidi, V.; Carotta, M. C.; Ferroni, M.; Martinelli, G.; Paglialonga, L.; Comini, E.; Sberveglieri, G. *Sens. Actuator B−Chem.* **1999**, *57*, 197−200.
(17) Stark, W. J.; Pratsinis, S. E.; Baiker, A. *Chimia* **2002**, *56*, 485−489.
(18) Zhang, Z. B.; Wang, C. C.; Zakaria, R.; Ying, J. Y. *J. Phys. Chem. B* **1998**, *102*, 10871−10878.
(19) Fuerte, A.; Hernandez-Alonso, M. D.; Maira, A. J.; Martinez-Arias, A.; Fernandez-Garcia, M.; Conesa, J. C.; Soria, J. *Chem. Commun.* **2001**, 2718−2719.
(20) Andersson, M.; Osterlund, L.; Ljungstrom, S.; Palmqvist, A. *J. Phys. Chem. B* **2002**, *106*, 10674−10679.
(21) Meng, Q. B.; Fu, C. H.; Einaga, Y.; Gu, Z. Z.; Fujishima, A.; Sato, O. *Chem. Mater.* **2002**, *14*, 83−88.
(22) Frindell, K. L.; Bartl, M. H.; Popitsch, A.; Stucky, G. D. *Angew. Chem.-Int. Ed.* **2002**, *41*, 959−962.
(23) Hagfeldt, A.; Grätzel, M. *Acc. Chem. Res.* **2000**, *33*, 269−277.
(24) Special Issue on "Sol−Gel Processed TiO_2-Based Materials for Solar Cells, Photocatalysts and other Applications" *J. Sol-Gel Sci. Technol.* **2001**, *22*, 5−179.
(25) Feldmann, C. *Adv. Mater.* **2001**, *13*, 1301−1303.
(26) Niederberger, M.; Bartl, M. H.; Stucky, G. D. *J. Am. Chem. Soc.* **2002**, *124*, 13642−13643.
(27) Niederberger, M.; Bartl, M. H.; Stucky, G. D. *Chem. Mater.* **2002**, *14*, 4364−4370.
(28) Scolan, E.; Sanchez, C. *Chem. Mater.* **1998**, *10*, 3217−3223.
(29) Guerrero, G.; Mutin, P. H.; Vioux, A. *Chem. Mater.* **2001**, *13*, 4367−4373.
(30) Ramakrishna, G.; Ghosh, H. N. *Langmuir* **2003**, *19*, 505−508.
(31) Roux, S.; Soler-Illia, G. J. A. A.; Demoustier-Champagne, S.; Audebert, P.; Sanchez, C. *Adv. Mater.* **2003**, *15*, 217−221.
(32) Kickelbick, G.; Holzinger, D.; Brick, C.; Trimmel, G.; Moons, E. *Chem. Mater.* **2002**, *14*, 4382−4389.
(33) Rajh, T.; Chen, L. X.; Lukas, K.; Liu, T.; Thurnauer, M. C.; Tiede, D. M. *J. Phys. Chem. B* **2002**, *106*, 10543−10552.
(34) Dimitrijevic, N. M.; Saponjic, Z. V.; Bartels, D. M.; Thurnauer, M. C.; Tiede, D. M.; Rajh, T. *J. Phys. Chem. B.* **2003**, *107*, 7368−7375.
(35) Moser, J.; Punchihewa, S.; Infelta, P. P.; Grätzel, M. *Langmuir* **1991**, *7*, 3012−3018.
(36) McWhirter, M. J.; Bremer, P. J.; Lamont, I. L.; McQuillan, A. J. *Langmuir* **2003**, *19*, 3575−3577.
(37) Cölfen, H.; Pauck, T. *Colloid Polym. Sci.* **1997**, *275*, 175−180.
(38) Börger, L.; Cölfen, H.; Antonietti, M. *Colloid Surf. A−Physicochem. Eng. Asp.* **2000**, *163*, 29−38.

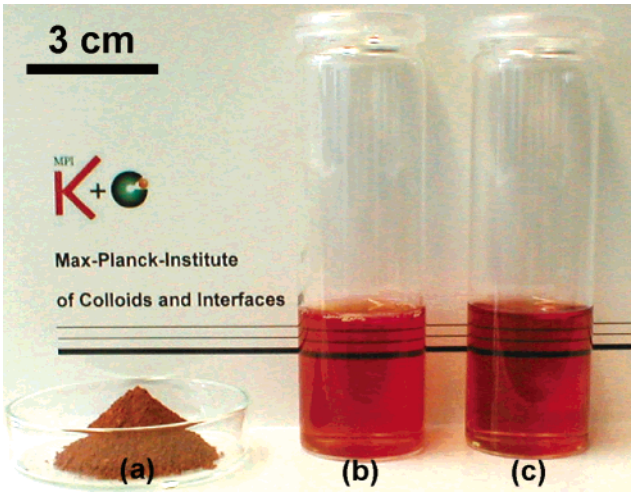

Figure 1. (a) Photograph of the as-synthesized isolated dopamine-modified titania powder, (b) aqueous solution of dopamine-modified titania nanoparticles, and (c) solution of 4-*tert*-butylcatechol-functionalized titania nanoparticles in a 0.001 M solution of TOPO in THF.

trioctylphosphine oxide (TOPO) to the THF solvent (10^{-3} M) enhances the solubility as well as the stability of the resulting clear, transparent solution (Figure 1c). The deep red color of both solutions arises from the ligand-to-metal charge-transfer interaction between the ligand and surface metal atoms.[33,35]

The solubility properties and the crystallinity of the functionalized nanoparticles are mainly determined by two reaction parameters, namely by the titanium chloride-to-ligand ratio and by the reaction temperature. Crystalline and water-soluble titania nanoparticles were obtained with a molar Ti-to-dopamine ratio ranging from 12 to 16 at a reaction temperature of 80 °C. Higher amounts of dopamine, i.e., Ti-to-dopamine ratios smaller than 10, decreased the crystallinity of the nanoparticles considerably. At reaction temperatures higher than 100 °C, the obtained dopamine-functionalized particles were no longer resoluble in water, even at a Ti-to-dopamine ratio of 5, due to increased agglomeration at higher temperature. In the case of 4-*tert*-butylcatechol, the amount of ligand has to be higher compared to the case of dopamine to provide good solubility. The initial molar ratio of Ti to 4-*tert*-butylcatechol was varied from 5 to 20. The best solubility in THF along with good crystallinity was obtained for ratios of 9−10 at a reaction temperature of 70 °C. At higher ratios, the particles also exhibit poor crystallinity. As crystallinity and solubility depend on the amount of ligand in an inverse fashion, an optimum had to be elaborated to ensure high crystallinity and solubility.

It is possible to estimate the surface coverage of the titania nanoparticles with dopamine. Rajh et al.[11] reported that the molar concentration of the titania surface sites can be calculated as follows: $[Ti_{surf}] = [TiO_2]12.5/d$, with $[TiO_2]$ being the molar concentration and d the diameter of the particles in angstroms. With a mean particle diameter of 55 Å (see below), the fraction of surface TiO_2 is approximately 23%. Since the applied Ti-to-dopamine ratio is only 16, and assuming that all the $TiCl_4$ is transformed into TiO_2 and all the dopamine molecules are linked to titania nanoparticles, the coverage of the particles with dopamine is only about 27%. Nevertheless, this is enough to provide good solubility of the particles in water.

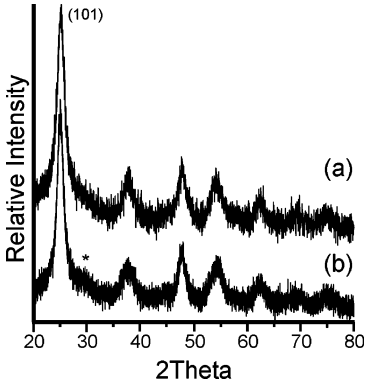

Figure 2. XRD powder patterns of nanocrystalline anatase samples prepared with (a) dopamine as surface modifier and (b) 4-*tert*-butylcatechol as ligand. Apart from the peak marked with *, all the peaks can be assigned to the anatase phase. The crystallite sizes were calculated from the broadening of the anatase (101) peak.

The X-ray powder diffraction pattern of dopamine-functionalized titania nanoparticles obtained at 80 °C with a Ti-to-dopamine ratio of 16 is shown in Figure 2a. All diffraction reflections can be assigned to the anatase phase without any indication of other crystalline polymorphs as byproducts. It is a notable feature that the particles exhibit such a good crystallinity, despite the low reaction temperature of 80 °C and the presence of the dopamine ligand. In the most cases, sol−gel processes lead to amorphous materials and subsequent heating is necessary to induce crystallization. A first estimation of the particle size is possible by monitoring the width of the (101) XRD peak for anatase. Using Scherrer's equation to determine the average crystallite size by peak-broadening analysis, a nanocrystal size of about 4 nm was calculated. Figure 2b shows the XRD powder pattern of a 4-*tert*-butylcatechol-functionalized sample obtained at 70 °C with a Ti-to-ligand ratio of 10. In addition to the peaks of the anatase phase, there is a small broad shoulder on the higher angle side of the anatase (101) peak, which may be assigned to small amounts of either amorphous intermediates or brookite[39] present in the sample.

The thermogravimetric measurement (see Supporting Information) of a dopamine-modified sample prepared at 80 °C with a Ti-to-dopamine ratio of 12 shows a considerable weight loss of approximately 27% in the range from room temperature to about 500 °C. The weight loss is a two-step process. The first step below 300 °C is due to the loss of adsorbed water and the residues of the organic solvent.[29] Above 300 °C the additional weight loss is about 13% relative to the weight of the starting material. This corresponds to 18 wt %, if the final weight of TiO_2 is chosen as a reference. Considering the starting concentrations of $TiCl_4$ and dopamine and assuming that all the $TiCl_4$ is transformed into TiO_2 and all the dopamine is adsorbed on the surface of the nanoparticles, the theoretical value of dopamine attached to the nanoparticles is about 16.5 wt %. The weight loss above 300 °C is mainly due to

(39) Pottier, A.; Cassaignon, S.; Chaneac, C.; Villain, F.; Tronca, E.; Jolivet, J.-P. *J. Mater. Chem.* **2003**, *13*, 877−882.

the degradation of the dopamine ligand and the removal of OH groups.[40,41] It was found that the dopamine-functionalized particles are rather hygroscopic. Particles that were stored in air for several days show a weight loss of more than 12% upon heating to 100 °C compared to a weight loss of 7% of the as-synthesized product in the same temperature range due to additional desorption of water. The BET surface area ranges from 122 m^2/g for the dopamine-functionalized nanoparticles (Ti-to-dopamine ratio of 16) to 210 m^2/g for the 4-*tert*-butylcatechol-functionalized nanoparticles (Ti-to-ligand ratio of 10).

Representative transmission electron micrographs of functionalized titania nanoparticles are shown in Figure 3. An overview image of dopamine-functionalized particles (Figure 3a) at low magnification illustrates that the sample entirely consists of nanosized titania particles arranged to a disordered thin film on the TEM grid, without the presence of larger particles or agglomerates. Crystallinity and phase are confirmed by electron diffraction analysis, revealing diffraction rings typical for the anatase phase (Figure 3a, inset). An image at higher magnification of the same sample (Figure 3b) shows sets of lattice fringes, giving additional evidence that the particles are highly crystalline. Although it is rather difficult to see the boundaries clearly, it can be said that the particles are quite uniform in size and shape. An estimation of the particle size is also possible. According to Figure 3b and the inset, the average particle size is approximately 5 nm, which is in good agreement with the data obtained from analytical ultracentrifugation (see below) and from XRD peak broadening. The particle size and crystallinity of the 4-*tert*-butylcatechol-functionalized particles are similar (Figure 3c).

For many applications of nanoparticles, particle size distribution is a fundamental parameter, but still its determination often remains a difficult task. Although TEM provides important information about the shape and size of individual nanoparticles, there is no unambiguous statistics for particle size distribution of the whole sample. Analytical ultracentrifugation (AUC) has proven to be a versatile tool for the measurement of the particle size distribution of colloidal samples.[37] In contrast to TEM, AUC detects all particles, even down to the smallest sizes. The resolution of the particle size distribution for small nanoparticles lies in the angstrom range.[37] The dopamine-functionalized titania nanoparticles synthesized at 80 °C with a Ti-to-dopamine ratio of 16 are a suitable model system for the particle size distribution measurement by AUC, because the particles exhibit good solubility in water and low agglomeration tendency. Furthermore, nanosized semiconductor titania shows a dependence of the band gap on the particle size, easily detected by the UV−vis absorption optics of the centrifuge. The particle size distribution is calculated by assuming a particle density of bulk anatase of 3.9 g/cm^3. This value is somewhat too high, since the dopamine ligand contributes considerably, but to an unkown extent, to the density of the

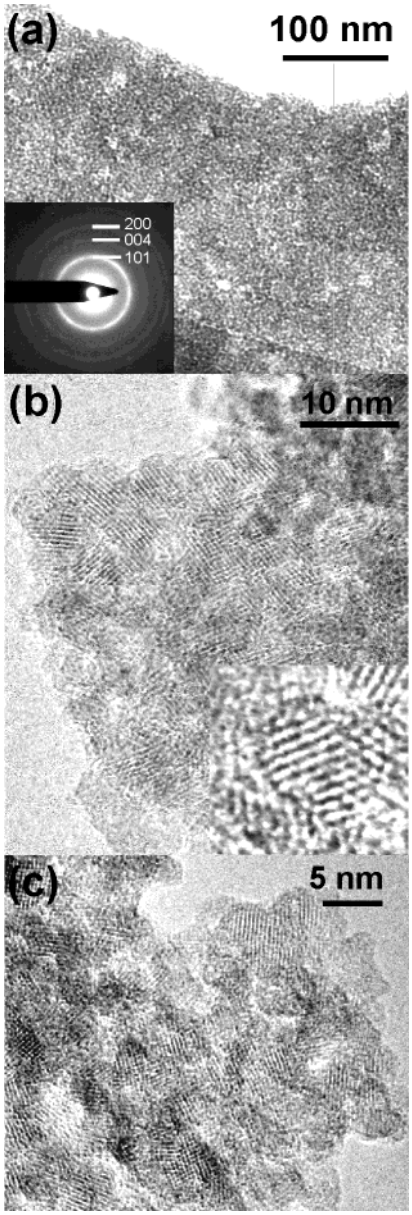

Figure 3. Representative TEM micrographs of as-synthesized functionalized titania nanoparticles. (a) An overview of dopamine-functionalized nanoparticles proves the exclusive presence of titania nanoparticles with an average diameter of about 5 nm. Inset: Selected area electron diffraction with diffraction rings corresponding to anatase. (b) Higher magnification TEM image of dopamine-functionalized nanoparticles demonstrating the crystalline nature of the nanoparticles. Inset: One particle with a diameter of about 5 nm. (c) Crystalline 4-*tert*-butylcatechol-functionalized nanoparticles with lattice fringes.

functionalized particles. The particle size distribution obtained from AUC ranges from about 3.5 to 8 nm, with a peak maximum at 5.5 nm (Figure 4, inset), proving that agglomeration of the particles in solution is negligible. Although already quite narrow, it has to be noted that this particle size distribution is broader than the real one, as diffusive peak broadening is not considered. The result agrees well with the particle sizes measured by TEM, speaking for the fact that neglected density correction due to the ligands in AUC and the invisibility of the ligands in TEM are counterbalancing approximations.

Nanosized semiconductor titania particles with sizes smaller than 3 nm show a dependence of the band gap

(40) Mueller, R.; Kammler, H. K.; Wegner, K.; Pratsinis, S. E. *Langmuir* **2003**, *19*, 160−165.
(41) Anpo, M.; Shima, T.; Kodama, S.; Kubokawa, Y. *J. Phys. Chem.* **1987**, *91*, 4305−4310.

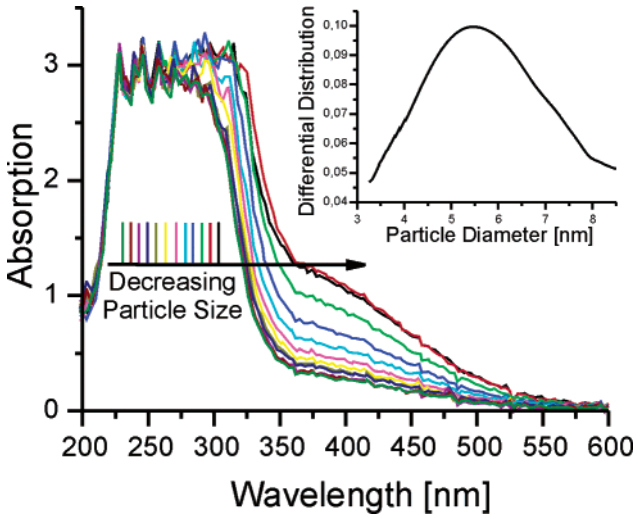

Figure 4. Results of the analytical ultracentrifugation measurements. UV−vis absorption spectra of dopamine-functionalized titania nanoparticles dependent on the particle size fractions. Inset: particle size distribution curve of dopamine-functionalized titania nanoparticles obtained at 80 °C with a Ti-to-dopamine ratio of 16.

energy on the particle size due to the quantum size effect.[42,43] AUC equipped with a UV−vis detector makes possible the measurement of the electronic absorption spectrum for each particle size fraction, resulting in a direct measurement of the absorption threshold dependent on the particle size (Figure 4). Interestingly, the dopamine-functionalized titania nanoparticles show a red shift of the UV absorption band with decreasing particle size. This behavior is opposed to the quantum size effect induced by the electron and hole confinement, which shifts the band gap of nanosized semiconductors to higher energies with reduced size.[44] However, the measured red shift agrees well with the results reported by Rajh et al., where smaller dopamine-functionalized titania nanoparticles also exhibit a red shift upon changing the particle size from 15 to 4.5 nm.[33] The red shift of the absorption is due to the surface complexation of the particles by enediol ligands. Light promotes electron transfer from the surface complexant to the conduction band of titania.[35] This effect is particularly pronounced in the present system, since the tail of the absorption band of dopamine-functionalized titania reaches far into the visible with an onset at around 550 nm. It was reported that the red shift is proportional to the fraction of the surface Ti atoms and correlates with the number of surface sites in nanocrystalline titania.[33] For example, dopamine-functionalized titania nanoparticles with full coverage of the surface show a red shift compared to nanoparticles with a surface coverage of 70%.[34] As a conclusion it can be said that with decreasing particle size the number of surface atoms increases, resulting in a red shift of the absorption band of the functionalized titania nanoparticles with decreasing particle size.

Although AUC generally allows the segregation of the sample into monodisperse fractions, it is not yet possible

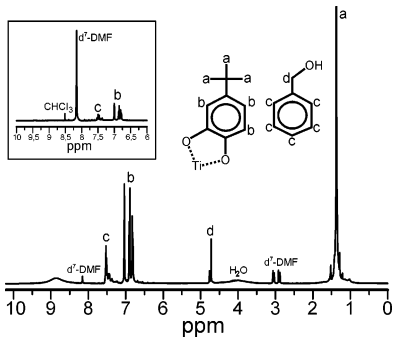

Figure 5. ^{1}H NMR spectrum of unwashed 4-*tert*-butylcatechol-functionalized titania nanoparticles dissolved in DMF-d_7 after an additional postsynthesis modification step in a highly concentrated 4-*tert*-butylcatechol/chloroform mixture. Inset: Carefully washed 4-*tert*-butylcatechol-functionalized titania nanoparticles dissolved in DMF-d_7 after an additional postsynthesis modification step in a 4-*tert*-butylcatechol/chloroform mixture with low ligand concentration.

to assign every single absorption spectrum exclusively to a specific particle size. The reason for this problem lies in uncontrolled diffusion processes, concentration, and charge effects. However, to the best of our knowledge, this is the first time that it was possible to measure the UV−vis spectra of semiconductor titania nanoparticles dependent on the particle size by fractionation of a preformed powder. In contrast to measurements on growing particles, which usually exhibit a large polydispersity, the use of analytical ultracentrifugation allows the measurement of almost monodisperse particle fractions.

Prior to ^{1}H NMR measurements, the concentration of surface-bound 4-*tert*-butylcatechol was increased by stirring as-prepared functionalized titania nanoparticles in solutions of 4-*tert*-butylcatechol in chloroform with different ligand concentrations. This procedure has several effects. First, the solubility of the titania particles in DMF as well as in chloroform is increased. While higher concentrations of 4-*tert*-butylcatechol lead to a homogeneous, completely transparent solution, the use of lower concentrations yields a milky dispersion in chloroform. However, after centrifugation, this precipitate is soluble in DMF. Second, a higher intensity of the 4-*tert*-butylcatechol signals in the NMR spectrum is obtained, and the usually very intense signals of benzyl alcohol are diminished. Figure 5 shows a ^{1}H NMR spectrum of 4-*tert*-butylcatechol-functionalized titania nanoparticles obtained by stirring in solution with a high ligand concentration. After evaporation of chloroform, the remaining titania nanoparticles functionalized with additional 4-*tert*-butylcatechol as well as unreacted ligand were dissolved in DMF-d_7. This spectrum was compared with ^{1}H NMR spectra obtained from measurements of the single components 4-*tert*-butylcatechol and benzyl alcohol in DMF-d_7 (data not shown). Pure 4-*tert*-butylcatechol gives rise to three signals at 1.4 ppm (*tert*-butyl group), 6.9−7.1 ppm (aromatic group), and 8.9 ppm (OH groups). In contrast to the spectrum of 4-*tert*-butylcatechol in $CDCl_3$, there is only one OH peak visible when measuring in DMF-d_7. The integral ratio of the peaks is 9.0:3.0:2.0. The signals are also present in the spectrum of the system containing functionalized nanoparticles and excess ligand (the *tert*-butyl group and the C_6H_3 group corresponding

(42) Kormann, C.; Bahnemann, D. W.; Hoffmann, M. R. *J. Phys. Chem.* **1988**, *92*, 5196−5201.
(43) Serpone, N.; Lawless, D.; Khairutdinov, R. *J. Phys. Chem.* **1995**, *99*, 16646−16654.
(44) Alivisatos, A. P. *J. Phys. Chem.* **1996**, *100*, 13226−13239.

to peaks a and b in Figure 5). No OH signals are expected from 4-*tert*-butylcatechol bound to the nanoparticles due to the deprotonation of the hydroxyl groups upon binding to the titanium atoms. As a matter of fact, the integral ratio in this spectrum is 10.0:3.0:1.2, indicating that almost half of the 4-*tert*-butylcatechol present in the system is coordinated to the titania particles (the slight intensity increase of the aliphatic peak originates from impurities). The presence of the broad OH peak at about 8.8 ppm is due to the excess of ligand and proves that the hydroxyl protons can, in principle, be detected in the system. H_2O adsorbed onto the surface of the particles is visible as a broad peak centered around 4.0 ppm. The benzyl alcohol signals appear at 7.5 ppm (C_6H_5 group, peak c) and 4.8 ppm (CH_2 group, peak d), giving evidence that still a considerable amount of benzyl alcohol is adsorbed on the surface of the functionalized nanoparticles. To prove the presence of the ligand on the titania, the nanoparticles were also stirred in less concentrated solutions of the ligand in $CHCl_3$. The particles were separated by centrifugation and they were washed thoroughly. The relevant low-field region of this spectrum is shown in Figure 5 (inset). The OH peak is completely absent; however, the aromatic signals of 4-*tert*-butylcatechol are clearly visible (inset, b). According to the integrals in the ^{1}H NMR spectrum (inset), the ratio of surface-adsorbed benzyl alcohol to 4-*tert*-butylcatechol is approximately 0.25, indicating that the coordination of 4-*tert*-butylcatechol is strongly preferred compared to the coordination of benzyl alcohol. This allows an increase of surface-bound 4-*tert*-butylcatechol in an efficient postsynthesis step.

Conclusion

Nanoengineering of particle surfaces is a key parameter for the design and construction of novel advanced materials. We present a ligand-assisted synthesis of well-defined anatase nanoparticles. In this context, three key observations are reported: (i) low-temperature and nonaqueous synthesis and in situ surface functionalization of crystalline anatase nanoparticles in form of an isolated powder; (ii) tailoring of the solubility properties by the choice of the appropriate ligand, resulting in high solubility of the powders in either water or organic solvents; (iii) due to the solubility of the particles, the use of AUC coupled with a UV−vis detector system is applicable, giving both statistical information about the particle size distribution in the whole sample as well as the dependence of physical properties such as band gap energy on well-defined particle sizes.

The existence of a highly crystalline and soluble titania powder which can be synthesized in a one-pot procedure at low temperatures and in gram quantities improves the accessibility, handling, and processability of this new precursor material. Furthermore, the use of enediol ligands such as dopamine is a particularly attractive route, since bifunctional ligands open the possibility for the covalent attachment of other organic electrophiles in a postsynthesis modification step, providing additional surface functionalization. This should have a high impact on diverse applications in photovoltaics, photocatalysis, and sensor technology and in the synthesis of composite materials.

Experimental Section

Materials. Titanium(IV) chloride (99.9%), benzyl alcohol (99.8%, anhydrous), 3-hydroxytyramine hydrochloride [dopamine, $(HO)_2C_6H_3CH_2CH_2NH_2\cdot HCl$] (98%), 4-*tert*-butylcatechol $(CH_3)_3CC_6H_3(OH)_2$ (97%), and trioctylphosphine oxide (TOPO) (99%) were obtained from Aldrich. All the chemicals were used without further purification.

Synthesis. In a typical synthesis, 160 mg (0.84 mmol) of 3-hydroxytyramine hydrochloride [or 250 mg (1.5 mmol) 4-*tert*-butylcatechol] were dispersed in 30 mL of benzyl alcohol in a glovebox. The vial was sealed and taken out of the box. 1.5 mL (13.6 mmol) of $TiCl_4$ was slowly added to the benzyl alcohol−ligand mixture under vigorous stirring at room temperature. **Caution should be taken as the reaction is rather violent.** Sometimes the dark red liquid contained some fluffy precipitate that completely dissolved again upon aging. The vial was sealed, and with continuous stirring the sol was heated to either 70 °C (4-*tert*-butylcatechol) or 80 °C (dopamine). The aging time was 2−5 days. The resulting brown suspension was centrifuged and the precipitate thoroughly washed twice with either chloroform in the case of the dopamine sample or methylene chloride in the case of the 4-*tert*-butylcatechol sample. After each washing step, the solvent was removed by centrifugation. The collected material was left to dry in air at room temperature and subsequently at 60 °C, yielding either a dark red powder in the case of the dopamine-functionalized nanoparticles or a brittle brown solid in the case of the 4-*tert*-butylcatechol-functionalized material.

Characterization. The X-ray powder diffraction (XRD) diagrams of all samples were measured in reflection mode (Cu Kα radiation) on a Bruker D8 diffractometer equipped with a scintillation counter. XRD patterns were obtained for 20°−80° 2θ by step-scanning with a step size of 0.01°. Transmission electron microscopy (TEM) investigations were performed either on an Omega 912 (Carl Zeiss) microscope, operated at 100 kV, or on a CM30 ST (Philips) microscope, operated at 300 kV (HRTEM). The samples were deposited onto a perforated carbon foil supported on a copper grid. Nitrogen adsorption and desorption isotherms of the functionalized titania particles were measured at 77 K with a Micromeritics Tristar 3000 system. Prior to the measurement, the sample was degassed at 150 °C overnight under vacuum. For the determination of the surface area, the BET method was used. A Netzsch thermoanalyzer TG 209 was used for the thermogravimetry measurement. Analytical ultracentrifugation was performed with a Beckman Optima XL-I centrifuge (Beckman/Coulter, Palo Alto, CA) with a scanning absorption optics and on-line Rayleigh interferometer. For the determination of the particle size distribution, the absorbance was measured at the two wavelengths of 400 and 450 nm at 10 000 rpm, 25 °C in a band centrifugation experiment to allow for an optimum particle separation. Here, 12 μL of the titania dispersion in water (ρ_{TiO_2} = 3.9 g/mL) was overlaid onto 300 μL of heavy water in a self-made 12 mm synthetic boundary Epon cell of the Vinograd type to avoid convection problems. The particle size distribution was calculated as published by assuming a spherical solid particle.[37] The UV−vis spectra were taken at radial positions where the local particle size was known from prior and subsequent radial scans. For the ^{1}H NMR measurements, about 200 mg of the wet titania particles functionalized with 4-*tert*-butylcatechol were redispersed in solutions of either 360 or 150 mg of 4-*tert*-butylcatechol in 20 mL chloroform and stirred at room temperature for 6 h. In the higher concentrated solution, the particles dissolved and could therefore not be separated by centrifugation. In this case, the solvent was evaporated and the sample dried overnight at room temperature. The ^{1}H NMR spectrum was measured after redissolving the obtained residue in dimethylformamide-d_7. The dispersion containing less 4-*tert*-butylcatechol remained milky, and the particles could be removed by centrifugation at 9000 rpm. The precipitate was washed three times with chloroform and subsequently dried overnight under vacuum at 60 °C. The powder was redissolved in dimethylformamide-d_7 or dimethyl sulfoxide-d_6 under slight sonication. The spectra were recorded

on a Bruker DPX400 spectrometer at 400 MHz, with a sample spinning rate of 20 Hz and a ZG30 pulse program.

Acknowledgment. We thank Antje Völkel for the AUC measurements. Financial support by the Max-Planck-Society is gratefully acknowledged.

Supporting Information Available: TGA measurements of dopamine-functionalized titania nanoparticles with a Ti-to-ligand ratio of 12. This material is available free of charge via the Internet at http://pubs.acs.org.

CM031108R